Physical Communication 8 (2013) 38–46

Contents lists available at ScienceDirect

Physical Communication

journal homepage: www.elsevier.com/locate/phycom

Full length article

A frequency domain multiple-antenna and channel estimation approach for facilitation of UWB technologies coexistence in heterogeneous WPANs

Abolfazl Mehbodniya[a,*], Wei Peng[a], Fumiyuki Adachi[a], Sonia Aïssa[b]

[a] Department of Electrical and Communication Engineering, Tohoku University, Sendai, Japan
[b] INRS-EMT, University of Quebec, Montreal, QC, Canada

ARTICLE INFO

Article history:
Received 30 October 2011
Received in revised form 25 July 2012
Accepted 15 August 2012
Available online 23 October 2012

Keywords:
Direct-sequence ultra wideband (DS-UWB)
Multiband orthogonal frequency division multiplexing (MB-OFDM)
Frequency domain equalization
Multiple-antenna
Channel estimation

ABSTRACT

Ultra wideband (UWB) communications is a promising technology which provides high data rates for short-range communications. There are currently two proposals as UWB standards, namely, multiband orthogonal frequency division multiplexing (MB-OFDM) UWB and direct-sequence (DS) UWB. These two standards can cause interference on each other and also to other wireless technologies when they are located in their vicinity. In this paper, we focus on the mutual interference of these two UWB standards. In the first part of the paper, we address the channel estimation issue for DS-UWB receiver, in the presence of multi-user interference (MUI) and MB-OFDM interference within the framework of wireless personal area networks (WPANs). In fact, we use the minimum mean square error estimation (MMSE) to estimate the channel based on a pilot transmission scheme. In the second part, we propose a simple but effective design for the receiver structure of the DS-UWB which utilizes a frequency domain multiple-antenna approach in order to mitigate MUI as well as the MB-OFDM external interference. Channel estimation performed in part one will be used in the detection process in part two. Numerical results are provided to evaluate the effectiveness of the proposed techniques for interference mitigation in DS-UWB.

1. Introduction

One of the newly emerged coexistence scenarios is between the two ultra wideband (UWB) standards. These standards, which have been proposed to the IEEE 802.15.3a task group, are multiband orthogonal frequency division multiplexing (MB-OFDM) UWB [1] and direct-sequence (DS) UWB [2]. The IEEE 802.15.3a task group could not finalize selection between these two standards. As a result, both standards will have to coexist together. Interference mitigation when these two technologies operate in the vicinity of each other is very challenging and appropriate solutions are yet to be developed. Previous research works on interference mitigation in UWB communication mainly address the narrowband interference (NBI) and propose techniques to reduce the NBI in UWB or vice versa [3–6]. However these technique may not be applicable for UWB interference on UWB, due to the large bandwidth of both systems. Another important issue which may affect the accuracy of the interference mitigation is the UWB channel estimation problem. Channel estimation becomes crucial in heterogeneous UWB environments where different sources of interference degrade the reference signal.

Previous works on channel estimation and interference mitigation between the aforementioned UWB standards are reported in [7–11]. In [7], the authors have derived

* Corresponding author.
E-mail addresses: mehbod@mobile.ecei.tohoku.ac.jp, a_mehbodniya@yahoo.com (A. Mehbodniya), peng@mobile.ecei.tohoku.ac.jp (W. Peng), adachi@ecei.tohoku.ac.jp (F. Adachi), aissa@emt.inrs.ca (S. Aïssa).

1874-4907/$ – see front matter © 2012 Elsevier B.V. All rights reserved.
doi:10.1016/j.phycom.2012.08.003

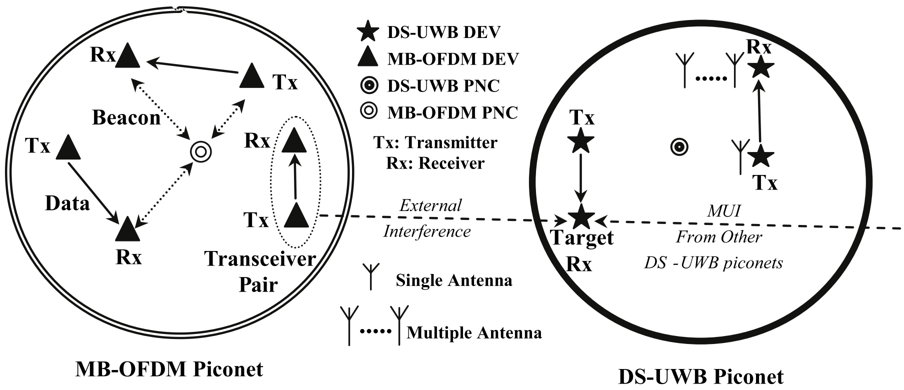

Fig. 1. A typical heterogeneous WPAN topology.

the channel parameter estimates using a maximum-likelihood (ML) approach. They have considered two different techniques for the channel estimation, i.e., data-aided and nondata-aided. This work solely focuses on channel estimation for one pulse position modulation (PPM) time-hopping (TH) UWB transceiver and does not take into account the effects of multi-user interference (MUI) and other external sources of interference. The work in [8] proposes a compressed sensing maximum likelihood (CSML) channel estimator in order to reduce the Nyquist sampling rate, which renders the implementation of UWB systems easier. The authors have shown that while retaining the noise statistics formulation of ML to achieve a reliable performance, the sampling rate is reduced significantly. However, similar to the previous work this work also focuses on single-user communications without considering different sources of interference. In [9], a waveforming technique has been proposed for the DS–UWB signal to mitigate the DS–UWB interference onto a MB-OFDM receiver which is in fact the reverse case scenario that we have considered in this work. In [10], the authors use a multi-carrier template waveform to mitigate the effect of MB-OFDM interference on a pulse-based UWB system (p-UWB); this work does not include an analytical modeling for the effect of MB-OFDM interference. A closer look at [10] also reveals that assuming a simple pulse model for an UWB system is not sufficient for studying the effect of interference on the UWB system as a victim receiver. On the other hand in the work reported in [11], the authors simulated the MB-OFDM UWB and DS–UWB standards to study the effect of the mutual interference between both systems, and proposed to reduce the interference by means of power control. This work solely focuses on UWB and neither considers any specific network topology as the target UWB application nor models the channel fading effect.

In this paper we address the coexistence issue of MB-OFDM and DS–UWB and we propose simple and innovative approaches for channel estimation and interference mitigation in this newly arisen coexistence scenario. In the first part, we present a channel estimation for the DS–UWB receiver within the novel framework of heterogeneous wireless personal area networks (WPANs). Specifically, we use a pilot-data transmission phase similar to the approach in [12] in order to estimate the UWB channel based on minimum mean square error estimation (MMSE). We consider the effect of internal interference or MUI caused by different transmitting DS–UWB systems and also the external interference caused by MB-OFDM transmitters. In the second part, we use the aforementioned channel estimation and we propose an interference mitigation technique for the DS–UWB system, when impaired by MUI and MB-OFDM interference (also called external interference). In fact, we have employed an adaptive multiple-antenna single carrier frequency domain (FD) equalization technique to mitigate the interference received by a DS–UWB receiver in WPANs. We show the effectiveness of our technique by providing the numerical results for the bit error rate (BER) of the DS–UWB system. We also investigate the performance of our method for different numbers of antennas in the DS–UWB receiver and different numbers of multiuser and MB-OFDM interferers. Results are obtained using two assumptions, i.e., having perfect channel state information (CSI) and partial CSI, where we use our approach to estimate the channel.

The remainder of this paper is organized as follows. In Section 2, the network topology and signals and channel models under study are provided. Section 3, addresses the interference analysis at the DS–UWB system. Section 4 explains our channel estimation method. Section 5, explains the DS–UWB receiver structure design and Section 6 presents numerical results and comparisons illustrating the BER performance of the DS–UWB system. Finally, concluding remarks are drawn in Section 5.

2. System model

In this section first we describe our network topology, then we present the models for the DS–UWB signal, MB-OFDM interfering signal and the channel, used in our study.

2.1. Network topology

In the heterogeneous coexistence environment, a number of nodes with different UWB technologies share the UWB spectrum. We consider the WPAN as network topology. Fig. 1 shows a typical heterogeneous WPAN topology consisting of two piconets. In the WPAN standard terminology, a piconet is a collection of nodes which

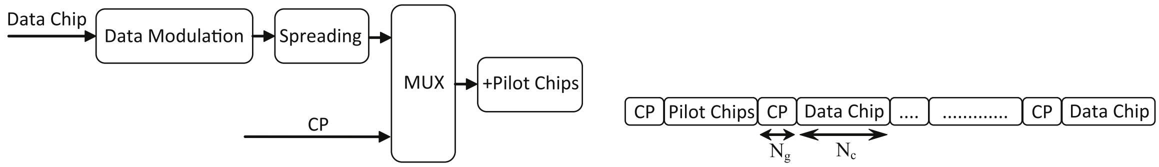

(a) Transmitter Structure. (b) Transmit Block Structure.

Fig. 2. Transmit block structure for DS–UWB.

form a network with the same technology. Each *node* is technically called a device (DEV). The piconet controller (PNC) is chosen by other DEVs and is responsible for coordinating and synchronizing the DEVs within the piconet. For this purpose PNC broadcasts *beacons* to the DEVs at regular superframe intervals. After coordination, the communication is performed directly between the transmitter and receiver, forming a *transceiver pair*. Here, we assume each receiver DS–UWB DEV is subject to external interference and MUI, i.e., interference from MB-OFDM DEVs and interference from other transmitter DS–UWB DEVs in other piconets. Due to synchronization of different transceiver pairs within a DS–UWB piconet by the PNC node, we do not consider the intra-piconet MUI. In our model, we also assume that the DS–UWB DEV uses a single antenna when it is in the transmission mode and uses multiple-antenna when it is in the receiver mode. The PNC of the piconet in which the target DS–UWB DEV is located, is assumed to exchange information with the PNC of other interfering MB-OFDM piconets in order to inform the target DS–UWB DEV about the frequency hopping pattern of interfering MB-OFDM DEVs.

2.2. Signals and channel models

The DS–UWB transmitted signal of the nth DEV within the nth DS–UWB piconet can be expressed as [9]:

$$s_{\mathrm{DS}}^{(n)}(t) = \sum_{s=0}^{N_c-1} d_n c_{s,n} q(t - sT_c), \tag{1}$$

where t is the time index and $q(t)$ is the pulse waveform and normalized such that $\int_{-\infty}^{+\infty} q^2(t)dt = 1$. N_c indicates the number of chips per information bit, the sequence $\{c_{s,n}\}$ represents the spreading signature, T_c denotes the hop width, $T_f = N_c T_c$ is defined as frame width and d_n represents the binary data transmitted.

For the nth MB-OFDM transmitter within the nth MB-OFDM piconet, the set of symbols $\{b_s^{(n)}, 0 \le s \le N-1\}$ are grouped into blocks which are modulated by an N-point IDFT (implemented with FFT) onto N subcarriers. The general formula for the transmitted symbol of the nth MB-OFDM transmitter at baseband is expressed as [9]:

$$B^{(n)}(t) = \sum_{s=0}^{N-1} b_s^{(n)} e^{\frac{j2\pi st}{T}}, \quad -T_G \le t \le T, \tag{2}$$

where T is the OFDM symbol duration and T_G is a guard interval, that is inserted to reduce the interference between blocks. $B^{(n)}(t)$ is assumed to be zero for $t < -T_G$ and $t \ge T$. At the RF block, a carrier is inserted and the signal is taken to the specified carrier frequency with respect to the frequency-hopping pattern of the MB-OFDM system:

$$\begin{aligned} s_{\mathrm{MB}}^{(n)}(t) &= \mathbf{Re}\left\{B^{(n)}(t)e^{j2\pi(f_c+f_{\mathrm{MB}})t}\right\} \\ &= \mathbf{Re}\left\{\sum_{s=0}^{N-1} b_s^{(n)} e^{j2\pi\left(\frac{s}{T}+f_c+f_{\mathrm{MB}}\right)t}\right\} \end{aligned} \tag{3}$$

where f_c is the constant carrier frequency offset for MB-OFDM and f_{MB} is the additive periodic value used to hop between the MB-OFDM frequency bands.

As for the channel, we consider the IEEE 802.15.3 standard's model [13]. The impulse response of the channel between nth DEV and the mth antenna of the target DS–UWB receiver is given by:

$$h_{n,m}(t) = \sum_{l=0}^{L-1} \sum_{u=0}^{U-1} h_{n,m,u,l}\,\delta(t - T_l - \tau_{u,l}), \tag{4}$$

where $h_{n,m,u,l} = p_{n,m,u,l}\beta_{n,m,u,l}$ is the gain coefficient of the uth ray in the lth cluster for the nth DEV at mth antenna, $p_{n,m,u,l}$ takes the values $+1$ or -1 with equal probability (to consider signal inversion because of reflections), $\beta_{n,m,u,l}$ is a lognormal random variable, $\tau_{n,m,u,l}$ is the arrival time of the uth ray with respect to the lth cluster arrival time (T_l), L denotes the number of clusters and U indicates the number of rays within each cluster. Here, we assume all the interferers experience the same fading condition.

Please note that $n = 0$ refers to our target DS–UWB transceiver pair under study which is located in 0th reference piconet and $n > 0$ refers to the nth interfering DS–UWB transmitter located in the nth piconet. We consider one DS–UWB interfering DEV at each piconet. As a result the reference index n for DEVs and piconets is identical. The same assumption stands for the index n referring to MB-OFDM external interfering DEVs.

3. Received signal analysis

In this section we present our transmitter structure for DS–UWB DEV, the received signal representation at the receiver DS–UWB DEV, as well as the analysis for different interference terms which are generated at the place of the receiver.

3.1. DS–UWB DEV transmitter structure

We consider a transmitter structure similarly to [14] for DS–UWB DEV as illustrated in Fig. 2(a). Binary data sequence is modulated, spread by spreading signature to form the data chip stream, which is then divided into a sequence of blocks of data chips with length N_c. We add a cyclic prefix (CP) to the beginning of each block, in order to suppress the inter block interference (IBI) caused by multi-path fading and large delay spread. The inserted CP is copied from the last N_g chips of each block. Usually, the length of CP is set to avoid IBI, thus longer than maximum channel delay. In addition, pilot chips are transmitted for channel estimation and adaptive weight control at the receiver. The frame structure of the transmitted block is shown in Fig. 2(b).

3.2. Received signal at the DS–UWB DEV receiver

With reference to the transmitter structure described in Section 3.1, the received chip block $\{r_m(t);\ t = 0 \sim N_c - 1\}$ of N_c symbols at the mth antenna of the target receiver DS–UWB DEV ($n = 0$) is given by

$$r_m(t) = \sum_{n=0}^{N_{\mathrm{DS}}-1} \sqrt{\frac{U_{\mathrm{P}}^{(n)}}{(D_{\mathrm{P}}^{(n)})^{\alpha}}} \sum_{l=0}^{L-1}\sum_{u=0}^{U-1} h_{n,m,u,l}\, s_{\mathrm{DS}}^{(n)} \times (t - T_l - \tau_{u,l}) + \sum_{n=0}^{N_{\mathrm{MB}}-1} \sqrt{\frac{U_{\mathrm{T}}^{(n)}}{(D_{T}^{(n)})^{\alpha}}} \sum_{l=0}^{L-1}\sum_{u=0}^{U-1} \times \tilde{h}_{n,m,u,l}\, s_{\mathrm{MB}}^{(n)}(t - T_l - \tau_{u,l}) + n_m(t) \tag{5}$$

where $U_{\mathrm{P}}^{(n)}$ denotes the transmitted signal's pulse energy of the nth DS–UWB DEV (and the bit energy will be $U_b^{(n)} = N_c U_{\mathrm{P}}^{(n)}$), α is the path loss exponent for UWB propagation, $D_{\mathrm{P}}^{(n)}$ is the contribution due to path loss which is proportional to the distance between the nth DS–UWB DEV and the target receiver and N_{DS} is the number of DS–UWB DEVs in other adjourning DS–UWB piconets which cause MUI to the target DS–UWB DEV ($n = 0$). $U_{\mathrm{T}}^{(n)}$ is the transmit symbol energy of the nth MB-OFDM transmitter, $D_T^{(n)}$ is the contribution due to path loss which is proportional to the distance between the nth interfering MB-OFDM DEV and the target receiver and N_{MB} is the number of MB-OFDM DEVs in other adjourning MB-OFDM piconets which cause External interference to the target DS–UWB DEV ($n = 0$). Please note that for simplification purposes we choose the length of the transmit block structure (FFT length) the same as the number of chips per information bits, N_c, in DS–UWB.

3.3. Multi-user interference (MUI) analysis

After passing through the correlation receiver, the output y_p corresponding to the pth path of the 0-th bit of the first DS–UWB receiver at the mth antenna is written as:

$$y_p = \sum_{w=p}^{p+N_c-1} \int_0^{T_f} r_m(t) c_{(w-p),0}\, q(t - wT_c)\,dt = \sqrt{\frac{U_{\mathrm{P}}^{(0)}}{(D_{\mathrm{P}}^{(0)})^{\alpha}}} d_1 h e^{j\tau} + I_{\mathrm{DS}}^{p} + I_{\mathrm{int}}^{p} + n_{\mathrm{DS}}^{p}, \tag{6}$$

where I_{DS}^{p} is the MUI, I_{int}^{p} is the contribution of the MB-OFDM interference and n_{DS}^{p} is the Gaussian noise with the variance $\sigma_{n_{\mathrm{DS}}}^2 = N_0 N_c/2$. Here we ignore the self-interference effect. The MUI can be written as:

$$I_{\mathrm{DS}}^{p} = \sum_{l=0}^{L-1}\sum_{u=0}^{U-1}\sum_{n=1}^{N_{\mathrm{DS}}-1} \sqrt{\frac{U_{\mathrm{P}}^{(n)}}{(D_{\mathrm{P}}^{(n)})^{\alpha}}} h_{n,m,u,l} e^{\tau_{n,m,u,l}} \sum_{w=p}^{p+N_c-1} \times \int_0^{T_f} s_{\mathrm{DS}}^{(n)}(t - (l-u)T_c) c_{(w-p),0}\, q(t - wT_c)\,dt. \tag{7}$$

I_{DS}^{p} in (7) can be further simplified according to [15]:

$$I_{\mathrm{DS}}^{p} = \sqrt{\frac{U_{\mathrm{P}}^{(n)}}{(D_{\mathrm{P}}^{(n)})^{\alpha}}} \sum_{l=0}^{L-1}\sum_{u=0}^{U-1}\sum_{n=1}^{N_{\mathrm{DS}}-1} h_{n,m,u,l} e^{\tau_{n,m,u,l}} \times \left(d_{-1}^{(n)} \bar{R}^{(n)}((l-u),p) + d_0^{(n)} R^{(n)}((l-u),p)\right), \tag{8}$$

where $\bar{R}$ and R are the partial cross-correlation functions and are defined as [15]:

$$R^{(n)}((l-u),p) = \int_0^{(l-u)T_c} C^{(n)}(t - (l-u)T_c) \times C^{(1)} q(t)\,dt. \tag{9}$$

$$\bar{R}^{(n)}((l-u),p) = \int_{(l-u)T_c}^{T_f} C^{(n)}(t - (l-u)T_c) \times C^{(1)}(t)\,dt. \tag{10}$$

In (9) and (10), $C^{(n)}(t)$ and $C^{(1)}(t)$ are given by

$$C^{(n)}(t) = \sum_{\nu=-\infty}^{\infty} c_{(\nu-(l-u))}^{(n)} q(t - \nu T_c). \tag{11}$$

$$C^{(1)}(t) = \sum_{\nu=-\infty}^{\infty} c_{(\nu-p)}^{(1)} q(t - \nu T_c). \tag{12}$$

The mean value of the real part of MUI is given by

$$\mathbf{E}[\mathbf{Re}[I_{\mathrm{DS}}^{p}]] = \sqrt{\frac{U_{\mathrm{P}}^{(n)}}{(D_{\mathrm{P}}^{(n)})^{\alpha}}} \sum_{l=0}^{L-1}\sum_{u=0}^{U-1}\sum_{n=1}^{N_{\mathrm{DS}}-1} \mathbf{E}[\mathbf{Re} \times [h_{n,m,u,l} e^{\tau_{n,m,u,l}}]](d_{-1}^{(n)} \bar{R}^{(n)}((l-u),p) + d_0^{(n)} R^{(n)}((l-u),p)), \tag{13}$$

where $\mathbf{E}\{\cdot\}$ denotes the expectation operation. $\mathbf{E}[\mathbf{Im}[I_{\mathrm{DS}}^{p}]]$ is calculated similar to $\mathbf{E}[\mathbf{Re}[I_{\mathrm{DS}}^{p}]]$. The covariance of I_{DS}^{p} is calculated according to

$$\mathrm{Cov}[\mathbf{Re}[I_{\mathrm{DS}}^{p_1}], \mathbf{Re}[I_{\mathrm{DS}}^{p_2}]] = \sqrt{\frac{U_{\mathrm{P}}^{(n)}}{(D_{\mathrm{P}}^{(n)})^{\alpha}}} \sum_{u=0}^{U-1} \sum_{\substack{l_1=0 \\ l_1 \neq p_1}}^{L-1} \sum_{\substack{l_2=0 \\ l_2 \neq p_2}}^{L-1} \sum_{n=1}^{N_{\mathrm{DS}}-1} \times \mathrm{Cov}[\mathbf{Re}[h_{n,m,u,l_1} e^{\tau_{n,m,u,l_1}}], \mathbf{Re}[h_{n,m,u,l_2} e^{\tau_{n,m,u,l_2}}]] \times \left(d_{-1}^{(n)} \bar{R}^{(n)}((l_1-u),p_1) + d_0^{(n)} R^{(n)}((l_1-u),p_1)\right) \times \left(d_{-1}^{(n)} \bar{R}^{(n)}((l_2-u),p_2) + d_0^{(n)} R^{(n)}((l_2-u),p_2)\right). \tag{14}$$

If we assume that multipath components for different transmitters are independent, the covariance term $\mathrm{Cov}[\mathbf{Re}[h_{n,m,u,l_1}e^{\tau_{n,m,u,l_1}}], \mathbf{Re}[h_{n,m,u,l_2}e^{\tau_{n,m,u,l_2}}]]$ in (14) is given by

$$\begin{aligned}&\mathrm{Cov}[\mathbf{Re}[h_{n,m,u,l_1}e^{\tau_{n,m,u,l_1}}], \mathbf{Re}[h_{n,m,u,l_2}e^{\tau_{n,m,u,l_2}}]]\\ &\quad= \mathrm{Cov}[\mathbf{Im}[h_{n,m,u,l_1}e^{\tau_{n,m,u,l_1}}], \mathbf{Im}[h_{n,m,u,l_2}e^{\tau_{n,m,u,l_2}}]]\\ &\quad= \begin{cases}\sigma^2_{n,m,u,l}, & \text{For } l_1 = l_2 = l\\ 0, & \text{For } l_1 \neq l_2.\end{cases}\end{aligned} \tag{15}$$

3.4. MB-OFDM interference analysis

By replacing (2) and (3) in (6) and applying some slight changes, the resulting interference term, I^p_{int}, at mth antenna is written as [16]:

$$\begin{aligned}I^p_{\mathrm{int}} &= \sum_{n=0}^{N_{\mathrm{MB}}}\sum_{w=p}^{p+N_c-1}\sqrt{\frac{U_{\mathrm{T}}^{(n)}}{(D_{\mathrm{T}}^{(n)})^{\alpha}}}\tilde{h}_{n,m,u,l}c_{(w-p),0}\\ &\quad\times\sum_{s=0}^{N-1}\mathbf{Re}\{b_s^{(n)}e^{j2\pi(s\Delta_F+f_c+f_{\mathrm{MB}})(wT_c-\tilde{\tau}_{n,m,u,l})}\\ &\quad\times\int_0^{T_c}e^{j2\pi(s\Delta_F+f_c+f_{\mathrm{MB}})x}q(x)dx\}\\ &= \sum_{n=0}^{N_{\mathrm{MB}}}\sum_{w=p}^{p+N_c-1}\sqrt{\frac{U_{\mathrm{T}}^{(n)}}{(D_{\mathrm{T}}^{(n)})^{\alpha}}}\tilde{h}_{n,m,u,l}c_{(w-p),0}\\ &\quad\times\sum_{s=0}^{N-1}\mathbf{Re}\left\{b_s^{(n)}e^{j\Upsilon(wT_c+\frac{T_p}{2}-\tilde{\tau}_{n,m,u,l})}Q(\Upsilon)\right\},\end{aligned} \tag{16}$$

where we can define $Q(\Upsilon) = \int_{-T_p/2}^{T_p/2}e^{j\Upsilon x}q(x)dx$ as the Fourier transform of the left-shifted version of pulse $q(t)$ which gives us a symmetric pulse and the limits of the integral have been changed to the pulse width of the signal, T_p. Eq. (16) can be simplified further as:

$$I^p_{\mathrm{int}} = \sum_{n=0}^{N_{\mathrm{MB}}}\sum_{w=p}^{p+N_c-1}\sum_{s=0}^{N-1}I_{w,s,n}, \tag{17}$$

where

$$\begin{aligned}I_{w,s,n} &= b_s^{(n)}\sqrt{\frac{U_{\mathrm{T}}^{(n)}}{(D_{\mathrm{T}}^{(n)})^{\alpha}}}\tilde{h}_{n,m,u,l}c_{(w-p),0}Q(\Upsilon)\\ &\quad\times\cos\left[\Upsilon\left(wT_c+\frac{T_p}{2}\right)\right].\end{aligned} \tag{18}$$

It is important to mention that (17) calculates the interference assuming all transmitters are transmitting at the same time. However, the total interference might be less depending on the network activity factor. Finally, n^p_{DS} is calculated as

$$n^p_{\mathrm{DS}} = \sum_{w=p}^{p+N_c-1}\int_0^{T_f}n(t)c_{(w-p),0}q(t-wT_c)dt. \tag{19}$$

4. Channel estimation

In order to estimate the UWB channel, we use a well known model similar to the one described in [12]. Please note that we use the bold text font to represent the arrays and the italic text font for the complex numbers. In this model, the fading amplitudes, $h_{m,n,l}$ are modeled as Rice variables and $h_{m,n,l}e^{j\tau_{m,n,l}}$ are complex Gaussian variables with independent quadrature components. During the pilot transmission a number of N_p identical bits are transmitted from the DS–UWB transmitter to the receiver and the correlators' output pertaining to $l = 0,\dots,L-1$ paths of the mth antenna is given by

$$\begin{aligned}\mathrm{T}^m &= \left[\mathbf{Re}[T_0^m]\mathbf{Im}[T_0^m]\ \cdots\ \mathbf{Re}[T_{L-1}^m]\mathbf{Im}[T_{L-1}^m]\right]\\ &= \sqrt{\frac{U_b^{(0)}N_pN_c}{(D_{\mathrm{T}}^{(0)})^{\alpha}}}\mathbf{h}+\mathbf{I}^p_{\mathrm{DS}}+\mathbf{I}^p_{\mathrm{int}}+\mathbf{n}^p_{\mathrm{DS}},\end{aligned} \tag{20}$$

where $\mathbf{h} = he^{\tau}$ and $\mathbf{I}^p_{\mathrm{DS}}$ is the MUI vector defined as

$$\mathbf{I}^p_{\mathrm{DS}} = \left[\mathbf{Re}[I^0_{\mathrm{DS}}]\ \mathbf{Im}[I^0_{\mathrm{DS}}]\ \cdots\mathbf{Re}[I^{L-1}_{\mathrm{DS}}]\ \mathbf{Im}[I^{L-1}_{\mathrm{DS}}]\right] \tag{21}$$

and the terms, $\mathbf{I}^p_{\mathrm{int}}$ and $\mathbf{n}^p_{\mathrm{DS}}$ are respectively, the MB-OFDM interference vector and thermal noise vector, which are defined similar to $\mathbf{I}^p_{\mathrm{DS}}$. The mean value vector and the covariance matrix of T^m is given by

$$\mathbf{E}[\mathrm{T}^m] = \sqrt{\frac{U_b^{(0)}N_pN_c}{(D_{\mathrm{T}}^{(0)})^{\alpha}}}\mathbf{E}[\mathbf{h}]+\mathbf{E}[\mathbf{I}^p_{\mathrm{DS}}]. \tag{22}$$

$$\begin{aligned}\mathrm{Cov}[\mathrm{T}^m] &= \frac{U_b^{(0)}N_pN_c}{(D_{\mathrm{T}}^{(0)})^{\alpha}}\mathrm{Cov}[\mathbf{h}]+\mathrm{Cov}[\mathbf{I}^p_{\mathrm{int}}]+\mathrm{Cov}[\mathbf{n}^p_{\mathrm{DS}}]\\ &\quad+\sqrt{\frac{U_b^{(0)}N_pN_c}{(D_{\mathrm{T}}^{(0)})^{\alpha}}}\mathrm{Cov}[\mathbf{h},\mathbf{I}^p_{\mathrm{DS}}]\\ &\quad+\sqrt{\frac{U_b^{(0)}N_pN_c}{(D_{\mathrm{T}}^{(0)})^{\alpha}}}\mathrm{Cov}[\mathbf{I}^p_{\mathrm{DS}},\mathbf{h}]+\mathrm{Cov}[\mathbf{I}^p_{\mathrm{DS}}].\end{aligned} \tag{23}$$

In (23), the terms, $\mathrm{Cov}[\mathbf{I}^p_{\mathrm{DS}}]$ and $\mathrm{Cov}[\mathbf{h}]$, are calculated using expressions in (14) and (15). The other terms can be derived easily with similar procedures. We use MMSE to estimate the channel, $\mathbf{h}$, in (20) based on the observation of the pilot vector T^m according to

$$\begin{aligned}\hat{\mathbf{h}} &= \mathbf{E}[\mathbf{h}|\mathrm{T}^m] = \left(\mathrm{Cov}[\mathbf{h},\mathrm{T}^m]\mathrm{Cov}^{-1}[\mathrm{T}^m]\right)\mathrm{T}^m\\ &\quad+\mathbf{E}[\mathbf{h}]-\mathrm{Cov}[\mathbf{h},\mathrm{T}^m]\mathrm{Cov}^{-1}[\mathrm{T}^m]\mathbf{E}[\mathrm{T}^m].\end{aligned} \tag{24}$$

It can be shown that

$$\mathrm{Cov}[\mathbf{h},\mathrm{T}^m] = \sqrt{\frac{U_b^{(0)}N_pN_c}{(D_{\mathrm{T}}^{(0)})^{\alpha}}}\mathrm{Cov}[\mathbf{h}]+\mathrm{Cov}[\mathbf{h},\mathbf{I}^p_{\mathrm{DS}}]. \tag{25}$$

This information will later be used to derive the optimum weights in FD adaptive antenna DS–UWB receiver design.

5. FD adaptive antenna receiver design

In this section we present the FD representation of the signal along with the structure design for the DS–UWB Receiver.

5.1. FD signal representation

Considering a half wavelength separation for the antenna array, the FD representation of (5) at the mth antenna on the kth frequency is given by:

$$R_m(k) = \sum_{n=0}^{N_{\mathrm{DS}}-1} H_{n,m}(k) S_{\mathrm{DS}}^{(n)}(k) + \sum_{n=0}^{N_{\mathrm{MB}}-1} \tilde{H}_{n,m}(k)\, S_{\mathrm{MB}}^{(n)}(k) + N_m(k), \qquad (26)$$

where

$$H_{n,m}(k) = \sum_{l=0}^{L-1}\sum_{u=0}^{U-1} h_{n,m,u,l}\, e^{\frac{-j2\pi k(T_l - \tau_{n,m,u,l})}{N_c T_c}} \qquad (27)$$

$$\tilde{H}_{n,m}(k) = \sum_{l=0}^{L-1}\sum_{u=0}^{U-1} \tilde{h}_{n,m,u,l}\, e^{\frac{-j2\pi k(T_l - \tilde{\tau}_{n,m,u,l})}{N_c T_c}}. \qquad (28)$$

Assuming that the chip sequence in (1) is aligned into a parallel buffer, the DFT of $s_{\mathrm{DS}}^{(n)}(t)$ is given by

$$S_{\mathrm{DS}}^{(n)}(k) = \sum_{t=0}^{N_c-1} d_n c_{t,n} q(t) e^{\frac{-j2\pi kt}{N_c T_c}} \qquad (29)$$

and

$$S_{\mathrm{MB}}^{(n)}(k) = \mathbf{Re}\left\{ \sqrt{U_{\mathrm{T}}^{(n)}} \sum_{t=0}^{N_c-1}\sum_{s=0}^{N-1} b_s^{(n)} e^{-j2\pi k \frac{t}{N_c T_c}} e^{j2\pi\left(\frac{s}{T} + f_c + f_{\mathrm{MB}}\right)t} \right\}. \qquad (30)$$

The FD received signal vector on the kth frequency is then expressed as

$$\mathbf{R}(k) = \sum_{n=0}^{N_{\mathrm{DS}}-1} \mathbf{H}_n(k) S_{\mathrm{DS}}^{(n)}(k) + \sum_{n=0}^{N_{\mathrm{MB}}-1} \tilde{\mathbf{H}}_n(k) S_{\mathrm{MB}}^{(n)}(k) + \mathbf{N}(k) \qquad (31)$$

with

$$\mathbf{H}_n(k) = \left[H_{n,0}(k) H_{n,1}(k) \cdots H_{n,N_r-1}(k)\right]^T, \qquad (32)$$

and

$$\mathbf{R}(k) = \left[R_0(k) R_1(k) \cdots R_{N_r-1}(k)\right]^T, \qquad (33)$$

where N_r is the number of antennas at the target DS–UWB DEV receiver.

5.2. DS–UWB DEV receiver design

The structure of FD receiver is shown in Fig. 3. A FD adaptive multiple-antenna weight control is applied on each frequency, then the output result of all the frequencies are summed up and a decision is made after the total result is brought back to the time domain.

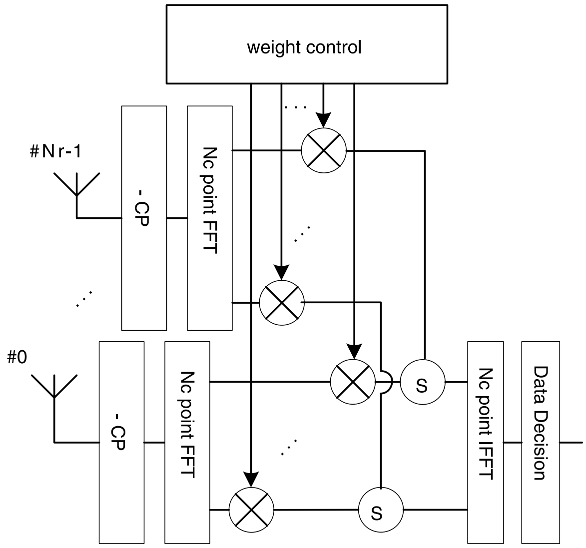

Fig. 3. FD receiver structure for DS–UWB.

Given the FD received signal in (5), weight control is performed as

$$\hat{\mathbf{R}}(k) = \mathbf{W}_{\mathrm{FD}}^T(k)\, \mathbf{R}(k) \qquad (34)$$

where $\mathbf{W}_{\mathrm{FD}}(k) = \left[W_{\mathrm{FD},0}(k), \ldots, W_{\mathrm{FD},N_r-1}(k)\right]^T$ is the FD weight control vector.

The FD weight is designed to minimize the mean squared error (MSE) between the FD output and the reference signal (in this study the pilot sequence is used as the reference signal to calculate the weights). Taking $S_{\mathrm{DS}}^{(0)}$ as the reference signal, the MSE is given by

$$\begin{aligned}\mathbf{E}\left\{e^2(k)\right\} &= \mathbf{E}\Big\{[S_{\mathrm{DS}}^{(0)}(k) - \mathbf{W}_{\mathrm{FD}}^T(k)\mathbf{R}(k)]^* \\ &\quad \times [S_{\mathrm{DS}}^{(0)}(k) - \mathbf{W}_{\mathrm{FD}}^T(k)\mathbf{R}(k)]\Big\} \\ &= \mathbf{E}\Big\{S_{\mathrm{DS}}^{(0)*}(k)S_{\mathrm{DS}}^{(0)}(k) - S_{\mathrm{DS}}^{(0)*}(k)\mathbf{W}_{\mathrm{FD}}^T(k)\mathbf{R}(k) \\ &\quad - \mathbf{R}^*(k)\mathbf{W}_{\mathrm{FD}}^H(k)S_{\mathrm{DS}}^{(0)}(k) \\ &\quad + \mathbf{R}^*(k)\mathbf{W}_{\mathrm{FD}}^H(k)\mathbf{W}_{\mathrm{FD}}^T(k)\mathbf{R}(k)\Big\} \end{aligned} \qquad (35)$$

$*$ is the conjugate operation and the superscript H represents the conjugate transpose operation. To minimize the MSE in (35), the FD weight must satisfy the following equality

$$\frac{\partial \mathbf{E}\left\{e^2(k)\right\}}{\partial \mathbf{W}_{\mathrm{FD}}(k)} = 0. \qquad (36)$$

Substituting (36) into (35), the following equality is obtained

$$\mathbf{E}\left\{-2S_{\mathrm{DS}}^{(0)}(k)\,\mathbf{R}^*(k) + 2\mathbf{R}^*(k)\,\mathbf{R}(k)\mathbf{W}_{\mathrm{FD}}(k)\right\} = 0. \qquad (37)$$

Hence, the FD weight vector $\mathbf{W}_{\mathrm{FD}}(k)$ is obtained as

$$\mathbf{W}_{\mathrm{FD}}(k) = \mathbf{C}_{rr}^{-1}(k)\,\mathbf{C}_{rd}(k) \qquad (38)$$

where

$$\mathbf{C}_{rd}(k) = E\left\{\mathbf{R}^*(k)\, S_0(k)\right\} = \mathbf{A}_0(k)\, S_0(k) \tag{39}$$

and

$$\begin{aligned}\mathbf{C}_{rr}(k) &= E\left\{\mathbf{R}^*(k)\,\mathbf{R}(k)\right\} \\ &= \mathbf{E}\left\{\mathbf{A}_0^*(k)\mathbf{A}_0(k) + \sum_{n=1}^{N_{\mathrm{DS}}-1}\mathbf{A}_n^*(k)\,\mathbf{A}_n(k) \right. \\ &\quad \left. + \sum_{n=0}^{N_{\mathrm{MB}}-1}\mathbf{F}_n^*(k)\mathbf{F}_n(k)\right\} + N_0\mathbf{I} \\ &= \mathbf{A}_0^*(k)\,\mathbf{A}_0(k) + \mathbf{R}_{NI}(k),\end{aligned} \tag{40}$$

where $\mathbf{A}_0(k) = \tilde{\mathbf{H}}_0(k)\, S_{\mathrm{DS}}^{(0)}(k)$ represents the propagation vector of the transmit signal from the desired DS–UWB DEV. $\mathbf{A}_n(k)$ is the propagation vector for MUI, $\mathbf{F}_n(k)$ is the propagation vector for the external MB-OFDM interference and N_0 denotes the power spectrum density of the AWGN. $\mathbf{I}$ is a $N_r \times N_r$ identity matrix, $\mathbf{R}_{NI}(k)$ is the auto-correlation matrix of the total interference plus noise and $\tilde{\mathbf{H}}_0$ is the estimate of the channel obtained in (24). We assume that the interference signals, the desired signal and the noise signal are uncorrelated.

The FD weight is then obtained by substituting (39) and the inverse of $C_{rr}(k)$ into (38) as

$$\mathbf{W}_{\mathrm{FD}}(k) = \left[\frac{1}{1 + \mathbf{A}_0(k)\mathbf{R}_{NI}^{-1}\mathbf{A}_0^*(k)}\right]\mathbf{R}_{NI}^{-1}(k)\,\mathbf{A}_0(k)S_0(k). \tag{41}$$

Finally the resultant signal in time domain is obtained by applying a N_d-point IFFT to $\hat{\mathbf{R}}(k)$ according to

$$\hat{d}(t) = \frac{1}{N_c}\sum_{k=0}^{N_c-1}\hat{\mathbf{R}}(k)\exp\left(-j2\pi k\frac{t}{N_cT_c}\right). \tag{42}$$

6. Numerical results

In our simulation we consider the BPSK modulation and the lower band spectrum for the DS–UWB DEVs in the range 3.1–4.85 GHz [2]. The MB-OFDM system utilizes 128 subcarriers, each with a spacing of 4.125 MHz. Three bands of operation are defined for a mode-1 device, with center frequencies at 3432 MHz, 3960 MHz and 4488 MHz. The MB-OFDM system hops between these three bands based on a special hopping sequence [1]. To simplify the simulation we approximate the UWB standard channel model with multipath Rayleigh fading similar to [17]. According to [1], the MB-OFDM system can tolerate a generic in-band modulated interferer with a power of $P_I > P_d - 9.0$ dB where P_I is the transmit power of MB OFDM DEVs and P_d is the transmit power of other system. In our simulation, unit transmit power of 0 dB is assumed for all the DS–UWB DEVs (either the target DS–UWB DEV or the multiuser interferers) and the transmit power of external interferers, MB OFDM DEV, varies in the range −9 to 0 dB. The noise power is set to −10 dB.

Fig. 4 shows the average BER performance of the target DS–UWB DEV versus the transmit power of interfering MB OFDM DEVs for $N_r = 4$ antennas at the receiver assuming perfect CSI. We considered the cases with one DS–UWB DEV ($N_{\mathrm{DS}} = 1$) and two DS–UWB DEVs ($N_{\mathrm{DS}} = 2$), while the number of MB OFDM DEVs is set to $N_{\mathrm{MB}} = 1$ and $N_{\mathrm{MB}} = 2$. Since no channel coding is assumed, we take the constant value, BER $= 10^{-2}$, as the target BER just as a reference point to be able to compare our different schemes. It is observed that one DS–UWB DEV and two MB OFDM DEVs can coexist when the MB OFDM DEV transmit power varies as −9 to 0 dB. Two DS–UWB DEVs and one MB OFDM DEV can coexist when the MB OFDM DEV transmit power is less than −5.3 dB and two DS–UWB DEVs and two MB OFDM DEVs can coexist when the MB OFDM DEV transmit power is less than −6 dB. It is also observed that increasing the number of MB OFDM DEVs (external interference) causes less degradation on the BER performance than increasing the number of DS–UWB DEVs (MUI). This can be justified by the frequency hopping of MB OFDM DEVs which only imposes a partial interference on the DS–UWB DEVs' bandwidth. As a result, the effect of the MB OFDM DEV interference is less significant than the DS–UWB DEV interference.

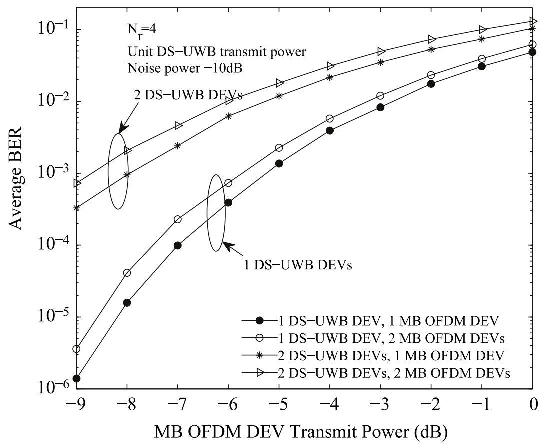

Fig. 4. Average BER of the target DS–UWB DEV versus the transmit power of the interfering MB OFDM DEVs for $N_r = 4$ (perfect CSI).

Fig. 5 derives the same results as in Fig. 4 but assuming partial CSI where the channel estimation technique proposed in Section 4 is used. It is observed that performance reduction, compared to the perfect CSI case, is about 0.8 dB.

Fig. 6 shows the average BER performance of the target DS–UWB DEV versus the transmit power of interfering MB OFDM DEVs for $N_r = 6$ antennas at the receiver assuming perfect CSI. Target BER is again kept as BER $= 10^{-2}$. It is observed that when the number of antennas is increased, the system can accommodate up to two DS–UWB DEVs and two MB OFDM DEVs while the MB OFDM DEV transmit power varies in the range −9 to 0 dB. The system can accommodate up to three DS–UWB DEVs and one MB OFDM DEVs when the MB OFDM DEV transmit power is less than −0.5 dB and up to three DS–UWB DEVs and two MB OFDM DEVs when the MB OFDM DEV transmit power is less than −0.8 dB.

Fig. 7 shows the similar results in Fig. 6, assuming partial CSI. Here, we notice a 0.8 dB reduction in BER

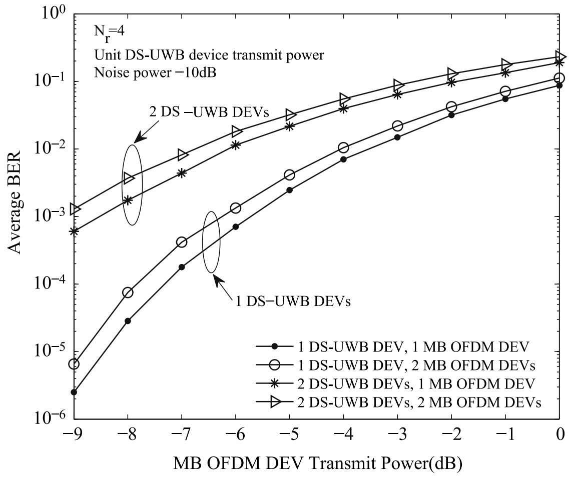

Fig. 5. Average BER of the target DS–UWB DEV versus the transmit power of the interfering MB OFDM DEVs for $N_r = 6$ and $\beta = 0.05$ (partial CSI).

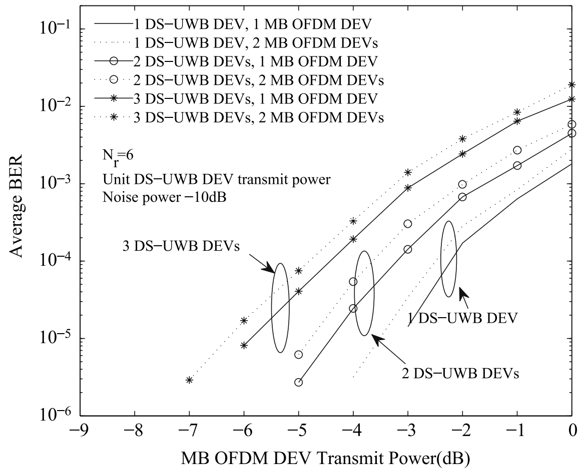

Fig. 6. Average BER of the target DS–UWB DEV versus the transmit power of the interfering MB OFDM DEVs for $N_r = 6$ (perfect CSI).

performance compared with the case where perfect CSI is available.

7. Conclusion

In this paper, the coexistence issue between MB-OFDM and UWB standards has been addressed. In order to mitigate the interference caused by MB-OFDM and DS–UWB devices on DS–UWB receiver, first we presented a channel estimation technique to estimate the propagation channel of the desired DS–UWB signal, then we proposed a frequency domain equalization with multiple-antenna for the DS–UWB receiver structure. A wireless personal area network was considered as the framework for our study. Simulation results revealed that our multiple-antenna approach can increase the capacity of the system and indirectly contribute to mitigating the interference induced onto the target DS–UWB DEV. It was also observed that the effect of external interference (originated by MB-OFDM) is less than multiuser interference (caused

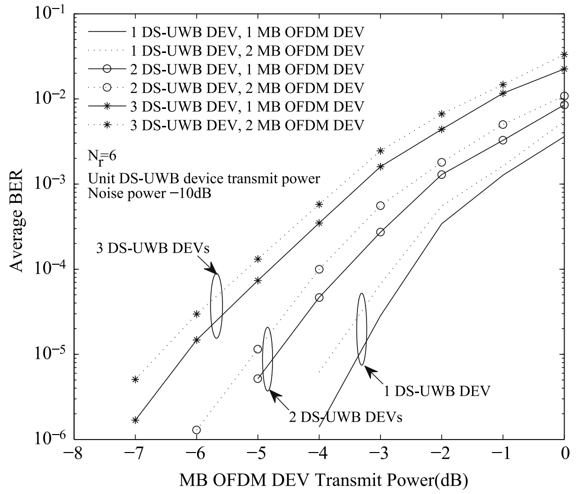

Fig. 7. Average BER of the target DS–UWB DEV versus the transmit power of the interfering MB OFDM DEVs for $N_r = 6$ and $\beta = 0.05$ (partial CSI).

by other simultaneous transmitting DS–UWB DEVs in other piconets). We also noticed a 0.8 dB reduction in BER performance when employing our channel estimation technique compared with the assumption of perfect CSI.

References

[1] A. Batra, J. Balakrishnan, A. Dabakand, et al. Multi-band OFDM physical layer proposal for IEEE 802.15 task group 3a, IEEE P802.15-03/268r3, March 2004.

[2] R. Fisher, R. Kohno, M. Mclaughlin, et al. DS-UWB physical layer submission to 802.15 task group 3a, IEEE P802.15-04/0137r4, January 2005.

[3] A. Mehbodniya, S. Aissa, Performance analysis of a 802.11a OFDM system in the presence of UWB and multipath interference, in: Proc. IEEE Sarnoff Symposium, May 2007, pp. 1–5.

[4] A. Giorgetti, M. Chiani, M.Z. Win, The effect of narrowband interference on wideband wireless communication systems, IEEE Trans. Commun. 53 (12) (2005) 2139–2149.

[5] R. Giuliano, F. Mazzenga, On the coexistence of power-controlled ultrawide-band systems with UMTS, GPS, DCS1800 and fixed wireless systems, IEEE Trans. Veh. Technol. 54 (1) (2005) 62–81.

[6] K.B. Letaief, N. Boubaker, MMSE multipath diversity combining for multi-access TH-UWB in the presence of NBI, IEEE Trans. Wireless Commun. 5 (4) (2006) 712–719.

[7] V. Lottici, A. D'fAndrea, U. Mengali, Channel estimation for ultra-wideband communications, IEEE J. Sel. Areas Commun. 20 (9) (2002) 1638–1645.

[8] T.-K. Liu, X. Dong, W. Lu, Compressed sensing maximum likelihood channel estimation for ultra-wideband impulse radio, in: Proc. IEEE International Conference on Communications, ICC'09, vol. 1, 2009, pp. 1–5.

[9] A. Mehbodniya, S. Aissa, Ultra wideband technologies coexistence in Nakagami-*m* fading channels, IET Commun. 3 (7) (2009) 1081–1088.

[10] K. Ohno, T. Ikegami, Interference mitigation study for UWB radio using template waveform processing, IEEE Trans. Microw. Theory Tech. 54 (4) (2006) 1782–1792.

[11] Y. Zhang, H. Wu, Q. Zhang, P. Zhang, Interference mitigation for coexistence of heterogeneous ultra-wideband systems, EURASIP J. Wireless Commun. Netw. (2006) 1–13.

[12] C.R.C.M. da Silva, L.B. Milstein, The effects of narrow-band interference on uwb communication systems with imperfect channel estimation, IEEE J. Sel. Areas Commun. 24 (4) (2006) 717–723.

[13] J. Foerester, et al. Channel modelling sub-committee report final, IEEE 802.15-02/490, November 2003.

[14] F. Adachi, H. Tomeba, K. Takeda, Frequency-domain equalization for broadband single-carrier multiple access, IEICE Trans. Commun. E92-B (5) (2009) 1441–1456.

[15] J. Lehnert, M. Pursley, Error probabilities for binary direct-sequence spread-spectrum communications with random signature sequences, IEEE Trans. Commun. 35 (1) (1987) 87–98.

[16] A. Mehbodniya, S. Aissa, Performance of DS-UWB in MB-OFDM and multi-user interference over Nakagami-*m* fading channels, Wiley Wireless Commun. Mobile Comput. (2011) First published online 18 January.

[17] Z. Qiyue, A. Tarighat, A. Sayed, Performance analysis of multiband OFDM UWB communications with application to range improvement, IEEE Trans. Veh. Technol. 56 (6) (2007) 3864–3878.

Abolfazl Mehbodniya received his Bachelor's degree and his Master's degree in Electrical Engineering from Ferdowsi University of Mashhad, Iran in 2002 and 2005 and his Ph.D.degree from the National Institute of Scientific Research-Energy, Materials, and Telecommunications (INRS-EMT), University of Quebec, Montreal, QC, Canada in 2010. Dr Mehbodniya is the recipient of the Japanese Society for the Promotion of Science (JSPS) Postdoctoral Fellowship and is currently a Research Fellow at the Graduate School of Engineering, Tohoku University. His research interests are in wireless communications, ultra wideband communications, interference management, radio resource management and cooperative relay networks.

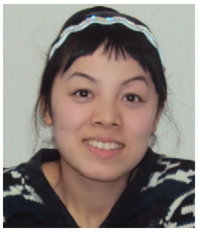

Wei Peng received her B.S and M.S degree in Electrical Engineering from Wuhan University, Wuhan, China, in 2000 and 2003 respectively. She received the Dr. Eng. degree in Electrical and Electronic Engineering from the University of Hong Kong, Hong Kong, in 2007. Since December 2007, she has been with the Department of Electrical and Communication Engineering, Tohoku University, where she is currently an Assistant Professor. Her research interests are in multiple antenna technology, single carrier transmission, and distributed antenna network.

Fumiyuki Adachi received the B.S. and Dr. Eng. degrees in Electrical Engineering from Tohoku University, Sendai, Japan, in 1973 and 1984, respectively. In April 1973, he joined the Electrical Communications Laboratories of Nippon Telegraph & Telephone Corporation (now NTT) and conducted various types of research related to digital cellular mobile communications. From July 1992 to December 1999, he was with NTT Mobile Communications Network, Inc. (now NTT DoCoMo, Inc.), where he led a research group on wideband/broadband CDMA wireless access for IMT-2000 and beyond. Since January 2000, he has been with Tohoku University, Sendai, Japan, where he is a Professor of Electrical and Communication Engineering at the Graduate School of Engineering. His research interests are in CDMA wireless access techniques, equalization, transmit/receive antenna diversity, MIMO, adaptive transmission, and channel coding, with particular application to broadband wireless communications systems. From October 1984 to September 1985, he was a United Kingdom SERC Visiting Research Fellow in the Department of Electrical Engineering and Electronics at Liverpool University. He is an IEICE Fellow and was a co-recipient of the IEICE Transactions best paper of the year award 1996, 1998, and 2009 and also a recipient of the Achievement award, 2003. He is an IEEE Fellow and was a co-recipient of the IEEE Vehicular Technology Transactions best paper of the year award in 1980 and again in 1990, and also a recipient of the Avant Garde award in 2000. He was a recipient of the Thomson Scientific Research Front Award, 2004, Ericsson Telecommunications Award 2008, and Telecom System Technology Award, 2010.

Sonia Aïssa received her Ph.D. degree in Electrical and Computer Engineering from McGill University, Montreal, QC, Canada, in 1998. Since then, she has been with the National Institute of Scientific Research-Energy, Materials, and Telecommunications (INRS-EMT), University of Quebec, Montreal, Canada, where she is currently a Full Professor. From 1996 to 1997, she was a Researcher with the Department of Electronics and Communications of Kyoto University, Kyoto, Japan, and with the Wireless Systems Laboratories of NTT, Kanagawa, Japan. From 1998 to 2000, she was a Research Associate at INRS-EMT, Montreal. From 2000 to 2002, while she was an Assistant Professor, she was a Principal Investigator in the major program of personal and mobile communications of the Canadian Institute for Telecommunications Research (CITR), leading research in radio resource management for code division multiple access systems. From 2004 to 2007, she was an Adjunct Professor with Concordia University, Montreal. In 2006, she was Visiting Invited Professor with the Graduate School of Informatics, Kyoto University, Japan. Her research interests lie in the area of wireless and mobile communications, and include radio resource management, performance evaluation, design and analysis of multiple antenna (MIMO) systems, and cross-layer design and optimization, with a focus on cellular, ad hoc, and cognitive radio networks.

Dr. Aïssa was the Founding Chair of the Montreal Chapter IEEE Women in Engineering Society in 2004–2007, a Technical Program Cochair for the Wireless Communications Symposium (WCS) of the 2006 IEEE International Conference on Communications (ICC 2006), and PHY/MAC Program Chair for the 2007 IEEE Wireless Communications and Networking Conference (WCNC 2007). She was also the Technical Program Leading Chair for the WCS of the IEEE ICC 2009, and is currently serving as Cochair for the WCS of the IEEE ICC 2011. She has served as a Guest Editor of the *EURASIP journal on Wireless Communications and Networking* in 2006, and as Associate Editor of the IEEE Wireless Communications Magazine in 2006–2010. She is currently an Editor of the IEEE Transactions on Wireless Communications, the IEEE Transactions on Communications and the IEEE Communications Magazine, and Associate Editor of the *Wiley Security and Communication Networks Journal*. Awards and distinctions to her credit include the Quebec Government FQRNT Strategic Fellowship for Professors and Researchers in 2001–2006; the INRS-EMT Performance Award in 2004 for outstanding achievements in research, teaching and service; the IEEE Communications Society Certificate of Appreciation in 2006 and 2009; and the Technical Community Service Award from the FQRNT Center for Advanced Systems and Technologies in Communications (SYTACom) in 2007. She is also co-recipient of Best Paper Awards from IEEE ISCC 2009, WPMC 2010 and IEEE WCNC 2010; and a recipient of the NSERC (Natural Sciences and Engineering Research Council of Canada) Discovery Accelerator Supplement Award.